DOCK8 Functions as an Adaptor that Links TLR–MyD88 Signaling to B Cell Activation

(Article begins on next page)

DOCK8 functions as an adaptor that links Toll-like receptor–MyD88 signaling to B cell activation

Haifa H. Jabara[1,15], **Douglas R. McDonald**[1,15], **Erin Janssen**[1], **Michel J. Massaad**[1], **Narayanaswamy Ramesh**[1], **Arturo Borzutzky**[1], **Ingrid Rauter**[1], **Halli Benson**[1], **Lynda Schneider**[1], **Sachin Baxi**[1], **Mike Recher**[1], **Luigi Notarangelo**[1], **Rima Wakim**[2], **Ghassan Dbaibo**[2], **Majed Dasouki**[3], **Waleed Al-Herz**[4], **Isil Barlan**[5], **Safa Baris**[5], **Necil Kutukculer**[6], **Hans Ochs**[7], **Alessandro Plebani**[8], **Maria Kanariou**[9], **Gerard Lefranc**[10], **Ismail Reisli**[11], **Kate Fitzgerald**[12], **Douglas Golenbock**[12], **John Manis**[13], **Sevgi Keles**[11,14], **Reuben Ceja**[14], **Talal Chatila**[14], and **Raif S. Geha**[1]

[1]Division of Immunology, Children's Hospital and Department of Pediatrics, Harvard Medical School, Boston, MA

[2]American University of Beirut, Beirut, Lebanon

[3]Departments of Pediatrics & Internal Medicine, Division of Genetics, Endocrinology & Metabolism, University of Kansas Medical Center, Kansas City, KS

[4]Allergy and Clinical Immunology Unit, Department of Pediatrics, Al-Sabah Hospital, Kuwait

[5]Division of Pediatric Allergy/Immunology, Marmara University, Istanbul, Turkey

[6]Department of Pediatric Immunology, Ege University, Izmir, Turkey

[7]Department of Pediatrics, University of Washington, Seattle, WA

[8]Department of Pediatric Hemato-Oncology, Spedali Civili, Brescia, Italy

[9]Agia Sophia Children's Hospital, Athens, Greece

[10]University of Montpellier, Montpellier, France

[11]Division of Pediatric Allergy and Immunology, Meram Medical Faculty, Selcuk University, Konya, Turkey

[12]University of Massachusetts, Worcester, MA

[13]Department of Transfusion Medicine, Children's Hospital, Boston, MA

[14]Division of Allergy and Immunology and Department of Pediatrics, University of California Los Angeles, Los Angeles, CA

Abstract

DOCK8 and MyD88 have been implicated in serologic memory. Here we report antibody responses were impaired and CD27^{+} memory B cells were severely reduced in DOCK8-deficient

patients. Toll-like receptor 9 (TLR9)- but not CD40-driven B cell proliferation and immunoglobulin production were severely reduced in DOCK8-deficient B cells. In contrast, TLR9-driven expression of *AICDA*, CD23 and CD86, and activation of NF-κB, p38 and Rac1 were intact. DOCK8 associated constitutively with MyD88 and the tyrosine kinase Pyk2 in normal B cells. Following TLR9 ligation, DOCK8 became tyrosine phosphorylated by Pyk2, bound the Src family kinase Lyn and linked TLR9 to a Src-Syk-STAT3 cascade essential for TLR9-driven B cell proliferation and differentiation. Thus, DOCK8 functions as an adaptor in a TLR9-MyD88 signaling pathway in B cells.

INTRODUCTION

Maintenance of serologic memory requires maturation of naïve B cells into memory B cells and long-lived plasma cells[1]. This involves interactions between ligand-receptor pairs that include CD40 ligand–CD40, BAFF or APRIL with TACI or BCMA, and TLR ligands–TLRs. TLR9 ligation on naïve B cells promotes proliferation, immunoglobulin secretion and maturation into memory B cells[2–4], and synergizes with CD40 and TACI in causing B cell activation[5, 6]. The TLR9 ligand CpG is an adjuvant for antibody responses in mice[7, 8]. Defective B cell responses to TLR9 ligation has been observed in patients with common variable immune deficiency characterized by poor antibody production and decreased generation of memory B cells and plasma cells[9].

Following ligand binding, TLR9 associates with and signals via the adaptor protein MyD88 (ref. 10). Resting B cells express several TLRs including TLR4 in mice and TLR6, 7, 9 and 10 in mice and humans. MyD88 is important for antibody responses to T dependent (TD) antigens administered with lipopolysaccharide (LPS) or CpG as adjuvants[11–13], although exceptions have been noted[14]. MyD88 does not appear to play a role in the antibody response to TD antigens administered with alum as adjuvant, or certain bacterial antigens[15–17], but is important for the antibody response to viruses[12, 18, 19].

The dedicator of cytokinesis-8 (DOCK8) is one of eleven members of the DOCK180 superfamily[20]. DOCK proteins have characteristic DOCK homology region-1 (DHR-1) and DHR-2 domains. The DHR-1 domain is important for DOCK protein targeting to membranes, through its binding of phosphatidylinositol (3,4,5)-triphosphate $(PtdIns(3,4,5)P_3)$[21]. The DHR2 domain binds to Rac-Rho family GTPases, and can function as an exchange factor for these GTPases[21]. The biological functions of DOCK8 include regulation of cell migration, morphology, adhesion and growth[20]. A mouse genetic screen for mutations that disrupt the persistence of the antibody response identified loss-of-function mutations in *Dock8* (ref. 23). DOCK8 mutant mice exhibit T cell lymphopenia, and their B cells fail to develop into marginal zone (MZ) B cells and to persist in germinal centers (GCs) and undergo affinity maturation. Reconstitution experiments indicate that DOCK8 expression in B cells is important for the normal persistence of GCs[22], suggesting that DOCK8 expression in B cells plays a key role in serologic memory.

Recently, mutations of *DOCK8* have been shown to account for a combined immunodeficiency in humans characterized by increased susceptibility to viral skin infections, severe allergy, elevated serum IgE, eosinophilia, T cell lymphopenia and impaired antibody responses[23, 24]. We analyzed the response of B cells from DOCK8-deficient patients to the TLR9 ligand CpG. DOCK8 was found to mediate a novel MyD88 signaling pathway, which is essential for TLR9-driven B cell proliferation and immunoglobulin production.

RESULTS

Antibody response and memory B cells in DOCK8 deficiency

Ten patients aged 3.5–15 years with homozygous mutations in *DOCK8* were studied (Supplementary Table 1). None had detectable DOCK8 protein in lysates of peripheral blood mononuclear cells (PBMCs) or Epstein-Barr virus (EBV) transformed B cells (data not shown). All had typical clinical characteristics of DOCK8 deficiency (Supplementary Table 2). Five patients, from whom serum was available prior to initiation of immunoglobulin replacement therapy, showed defective IgG antibody response to tetanus toxoid (TT), hepatitis B vaccine (Hep. B), TT-conjugated *Haemophilus influenzae* type B vaccine (HiB) and conjugated pneumococcal polyvalent vaccine (PV) (Table 1). The IgM TT antibody response was significantly decreased in these patients (Supplementary Fig. 1). Two of these patients, aged 8 and 15 years mounted a brisk early antibody response 8 weeks after a booster dose of TT, which fell below the protective level twelve and fifteen months later (Fig. 1a). This response is in contrast to >99% of normal children, in whom protective antibody titers persist five years after TT booster vaccination [25, 26].

Flow cytometry analysis of PBMCs revealed that the percentage of CD3^{+} T cells was significantly decreased in the patients compared to age-matched healthy controls, as previously reported[23, 24], while the percentage of CD19^{+} B cells was normal or increased (Fig. 1b). There was a severe deficiency in the percentage of circulating CD19^{+}CD27^{+} memory B cells in all patients examined, with CD19^{+}CD27^{−} naïve B cells accounting for virtually all (>95%) their B cells (Fig. 1c,d). The percentage of circulating IgD^{+}CD27^{+} MZ-like B cells was decreased in the patients compared to controls (Supplementary Fig. 2), consistent with the findings in DOCK8 mutant mice[22]. These results indicate that DOCK8 is important for the generation of memory B cells and serologic memory in humans.

Impaired B cell activation by CpG in DOCK8 deficiency

The TLR9 ligand CpG ODN 2006 (thereafter referred to as CpG) acts selectively on human B cells[27], and has no detectable effects on non-B cells[28]. PBMCs from DOCK8-deficient patients were severely deficient in their capacity to proliferate and to secrete IgM and IgG in response to CpG stimulation, compared to PBMCs from age-matched normal subjects, which included shipping controls (Fig. 2a). In contrast, DOCK8-deficient PBMCs proliferated and secreted IgM normally following stimulation with anti-CD40 plus interleukin 21 (IL-21), and secreted about half the amount of IgG as normal PBMCs (Fig. 2b). PBMCs from the patients proliferated and secreted IgE in response to anti-CD40 plus IL-4 to an extent comparable to normal PBMCs (Fig. 2c).

The severely impaired response of DOCK8-deficient PBMCs to CpG could not be simply explained by the lack of memory B cells. Highly purified naïve B cells from normal subjects (>95% CD27^{−}, Supplementary Fig. 3a), proliferated to CpG to an extent comparable to total B cells isolated from the same subjects (Fig. 2d). Consistent with previous reports[2–4], the amounts of IgM and IgG secreted by CpG-stimulated naïve B cells were reduced to respectively ~one-half and ~one-third of those secreted by CpG-stimulated total B cells (Fig. 2d). In contrast, purified B cells from DOCK8-deficient patients, which were virtually all naive, completely failed to proliferate and to secrete IgM and IgG in response to CpG (Fig. 2d). Proliferation and secretion of IgM and IgG in response to anti-CD40 plus IL-21 was comparable in normal naïve B cells and DOCK8-deficient purified B cells (Supplementary Fig. 3b). The decreased IgG secretion of DOCK8-deficient PBMCs to anti-CD40 plus IL-21 was most likely secondary to lack of memory B cells, because purified normal naïve B cells exhibited a comparable decrease in IgG secretion in response to anti-CD40 plus IL-21 relative to total B cells (Supplementary Fig. 3b). The failure of B cells from DOCK8-

deficient patients to respond to CpG was not due to increased apoptosis and cell death, as determined by staining with Annexin V and propidium iodide (Supplementary Fig. 4). These results indicate that B cells from DOCK8-deficient patients have an intrinsic and selective defect in their ability to respond to CpG.

CpG activates known pathways in DOCK8 deficient B cells

CpG stimulation of B cells induces the expression of *AICDA*, which encodes activation-induced cytosine deaminase (AID) that is critical for isotype switching, and upregulates the expression of the low affinity IgE receptor CD23 and the co-stimulatory molecule CD86 (refs. 4,29). CpG stimulation induced comparable *AICDA* mRNA expression in PBMCs and B cells from DOCK8-deficient patients and controls (Fig. 3a), and comparable increases in the percentage of CD19^{+} B cells that express CD23 and CD86 (Fig. 3b,c). The mean fluorescence intensity (MFI) of these antigens on B cells was comparable between DOCK8-deficient patients and controls (Fig. 3b,c). NF-κB and the MAP kinase p38 are activated by CpG stimulation and play an important role in the induction of *AICDA,* CD23 and CD86 expression[30–32]. CpG stimulation caused comparable IκBα and p38 phosphorylation in EBV-B cells and PBMCs from DOCK8-deficient patients and controls (Fig. 3d and data not shown). CpG-driven IL-6 secretion by EBV-B cells was not significantly different between patients and controls (Fig. 3e). CpG stimulation causes plasmacytoid dendritic cells (pDCs) to secrete interferon-α (IFN-α). This induction requires MyD88-dependent activation of IRF7 (ref. 33). Stimulation of PBMCs with the CpG type A ODN 2216, which activates TLR9 in human pDCs, resulted in comparable secretion of IFN-α in patients and controls (Fig. 3f)

The DHR2 domain of DOCK proteins can activate Rac and/or Cdc42 (ref. 21) and CpG activates Rac1 in DCs[34]. To examine Rac1 activation, a fusion protein of glutathione-S-transferase (GST) and the GTPase binding domain of p21-activated kinase (GST-PAK) was used to precipitate GTP-bound Rac1 and Cdc42 from cell lysates, followed by immunoblotting with antibodies to Rac1 and Cdc42. Stimulation with CpG resulted in comparable Rac1 activation in EBV-B cells from normal and DOCK8-deficient subjects (Fig. 3g), but caused no detectable Cdc42 activation (data not shown). Thus, CpG activates Rac1 in B cells, but DOCK8 is not essential for this activation.

DOCK8 dependent activation of STAT3 by CpG in B cells

STAT3 is important for B cell proliferation and differentiation in response to anti-CD40 plus IL-21 (ref. 35,36). Stimulation of normal PBMCs with CpG induced STAT3 phosphorylation on residue Y705 (Fig. 4a). In contrast, CpG-driven, but not IL-21-driven, STAT3 phosphorylation was defective in DOCK8-deficient PBMCs (Fig. 4a). CpG-driven, but not IFN-α induced, STAT3 phosphorylation was defective in purified DOCK8-deficient B cells (Fig. 4b), indicating that the defect is B cell autonomous. IL-6 and IL-21 caused comparable STAT3 phosphorylation in purified B cells from patients and controls (Fig. 4c). Densitometry scanning analysis demonstrated that CpG-driven STAT3 phosphorylation in B cells from DOCK8-deficient patients was 18±7% of control ($n = 3$ each, $P < 0.01$), whereas IL-21-driven STAT3 phosphorylation was comparable (Fig. 4d). The defect in CpG-driven STAT3 phosphorylation in DOCK8-deficient B cells was not secondary to lack of memory B cells, because CpG caused comparable STAT3 phosphorylation in purified naïve B cells and unfractionated B cells from normal controls (Fig. 4e). These results demonstrate that DOCK8 deficiency selectively impairs CpG-driven STAT3 phosphorylation in B cells.

The role of STAT3 in CpG-driven B cell proliferation and differentiation was investigated by examining PBMCs from six patients with autosomal dominant hyper-IgE syndrome (AD-HIES), resulting from different dominant-negative mutations in *STAT3* (Supplementary

Table 3). PBMCs from these patients had significantly impaired proliferation and IgG secretion following stimulation with CpG (Fig. 4f). There was no significant difference between PBMCs from AD-HIES patients and controls in their ability to proliferate and secrete IgE in response to anti-CD40 plus IL-4 (Fig. 4g). As previously reported[35], PBMCs from AD-HIES patients failed to proliferate and secrete IgG in response to anti-CD40 plus IL-21 (Supplementary Fig. 5).

Because IL-6 caused STAT3 phosphorylation in DOCK8-deficient B cells, we examined whether exogenous IL-6 corrects their defective response to CpG. Addition of rIL-6 to DOCK8-deficient PBMCs failed to correct their defective proliferation and IgG secretion in response to CpG (Fig. 4h, and data not shown). These results indicate that in addition to STAT3 phosphorylation, other signals that are important for CpG-driven B cell proliferation and differentiation are impaired in DOCK8-deficient B cells.

TLR9 protein expression was comparable in B cells from patients and controls (Supplementary Fig. 6a). Correct subcellular localization of TLR9 is essential for its function[37]. Lack of DOCK8 might result in TLR9 mislocalization, which could interfere with the ability of TLR9 to activate STAT3. EBV-B cells from normal subjects and DOCK8-deficient patients were stimulated for 90 min with CpG, permeabilized and simultaneously stained for TLR9 and either endoplasmic reticulum (ER Tracker®), the early endosomal marker EEA-1 or the late endosomal-lysosomal markers LAMP-1 (also known as CD107a). Fluorescent microscopy revealed that the subcellular localization of TLR9 was comparable in normal and DOCK8-deficient EBV-B cells (Supplementary Fig. 6b). Thus DOCK8 has no detectable role in TLR9 trafficking in B cells.

Syk is downstream of DOCK8 in CpG activated B cells

The tyrosine kinase Syk activates STAT3 in B lymphoma cells[38, 39]. Stimulation of normal PBMCs with CpG caused Syk phosphorylation on residue Y352, the target of Src kinases (Fig. 5a). In contrast, it caused negligible Syk phosphorylation in DOCK8-deficient PBMCs (Fig. 5a). The defect in Syk phosphorylation was specific to CpG because B cell receptor (BCR) crosslinking with anti-IgM caused comparable Syk phosphorylation in patients and controls (Fig. 5b). Densitometry scanning analysis demonstrated that CpG-driven Syk phosphorylation in PBMCs from DOCK8-deficient patients was $16\pm8\%$ of controls, ($n = 3$ each, $P < 0.001$), while BCR-driven Syk phosphorylation was not significantly different (Fig. 5c).

The pentapeptide Syk inhibitior SYKINH-61 was used to examine whether Syk activation is important for CpG-driven STAT3 phosphorylation. SYKINH-61 inhibited CpG-driven STAT3 phosphorylation in normal PBMCs ($85\pm5\%$ inhibition, $n = 3$), but had no effect on IL-21-driven STAT3 phosphorylation (Fig. 5d), or CpG-driven phosphorylation of p38 (data not shown). Moreover, SYKINH-61 inhibited CpG-driven proliferation and IgG production in normal PBMCs in a dose-dependent manner, but had no effect on CD40–IL-21-driven proliferation and IgG production (Fig. 5e,f).

The role of Syk in CpG-driven STAT3 phosphorylation was verified using RNA silencing. The mouse B cell line CH12 faithfully reproduced the response of primary human B cells to CpG stimulation by exhibiting Pyk2, Syk and STAT3 phosphorylation (Supplementary Fig. 7a). shRNA knockdown (KD) of Syk, but not introduction of non-silencing (NS) shRNA, strongly reduced Syk protein expression and strongly inhibited CpG-driven STAT3 phosphorylation in CH12 cells (Supplementary Fig. 7b–d). These results place Syk upstream of STAT3 activation by CpG in B cells.

CpG may bind to sensors other than TLR9 (ref. 34). To determine if DOCK8 dependent CpG-driven phosphorylation of Syk and STAT3 proceeds through the engagement of TLR9 and its adaptor protein MyD88, we compared the response of purified splenic B cells (>95% B220^{+} cells) from *Tlr9*^{−/−} and *Myd88*^{−/−} mice and their genetically matched wild-type controls. CpG stimulation resulted in the phosphorylation of Syk and STAT3 in B cells from wild-type mice (Fig. 5g,h), as in normal human B cells. In contrast, CpG stimulation caused minimal Syk and STAT3 phosphorylation in B cells from *Tlr9*^{−/−} and *Myd88*^{−/−} mice. Furthermore, CpG failed to cause proliferation and IgG secretion by B cells from *Tlr9*^{−/−} and *Myd88*^{−/−} mice (Supplementary Fig. 8). Together, these results indicate that CpG engages TLR9–MyD88 to cause DOCK8-dependent phosphorylation of Syk and STAT3, which is essential for B cell proliferation and differentiation.

CpG activates a Pyk2-Src-Syk-STAT3 cascade in B cells

Stimulation of normal PBMCs with CpG resulted in tyrosine phosphorylation of proteins with molecular weights that correspond to those of Src family kinases (54–56 kDa), their target Syk (72 kDa), and Pyk2 (110 kDa), a tyrosine kinase that functionally interacts with Src kinases (Fig. 6a). In contrast, it caused minimal protein tyrosine phosphorylation in PBMCs from DOCK8-deficient patients. This defect was selective to CpG stimulation, because BCR crosslinking caused comparable protein tyrosine phosphorylation in PBMCs from DOCK8-deficient patients and controls (data not shown), consistent with the normal activation of B cells from DOCK8 mutant mice following BCR crosslinking[22].

Pyk2 is auto-phosphorylated on tyrosine residue Y402 (ref. 40). Activated Src family kinases (thereafter referred to as Src) are autophosphorylated on Y residues that correspond to Y416 in Src[40], and are recognized by anti-pY416Src. Immunoblotting lysates of PBMCs with phosphospecific mAbs to pY402Pyk2 and pY416Src demonstrated that stimulation with CpG caused Pyk2 and Src phophorylation in normal PBMCs (Fig. 6b). In contrast, CpG stimulation caused minimal phosphorylation of Pyk2 and Src in DOCK8-deficient PBMCs (Fig. 6b), demonstrating that CpG-driven tyrosine phosphorylation of Pyk2 and Src is DOCK8 dependent. Pyk2 and Src were phosphorylated after CpG stimulation of B cells from wild-type, but not *Myd88*^{−/−} mice (Fig. 6c), indicating that TLR9-driven phosphorylation of Pyk2 and Src, like that of Syk and STAT3, is dependent on MyD88.

We used selective inhibitors of Pyk2 and Src to examine the roles of these kinases in CpG-driven activation of B cells. The Pyk2 inhibitor Tyrphostin A9 strongly inhibited CpG-driven tyrosine phosphorylation of Pyk2, Src, Syk and STAT3 (Fig. 6d-g). In three experiments the inhibition was 84±3% for Pyk2, 81±6% for Src, 95±4% for Syk and 97±2% for STAT3. Tyrphostin A9 had no detectable effect on IL-6 driven STAT3 phosphorylation, or CpG-driven p38 phosphorylation (data not shown). Tyrphostin A9 strongly inhibited CpG-driven IgG secretion by 90±2% ($n = 3$, $P < 0.01$), but not CD40–IL-21 driven IgG secretion (Fig. 6h). Similar results were obtained with the structurally different Pyk2 inhibitor PF562271 (data not shown). The role of Pyk2 in CpG-driven STAT3 phosphorylation was verified using shRNA knockdown in CH12 B cells (Supplementary Fig. 7b–d).

The Src inhibitor PP2 had a modest effect on CpG-driven Pyk2 phosphorylation (Fig. 6d), but more strongly inhibited CpG-driven phosphorylation of Src, Syk and STAT3 (Fig. 6e–g). In three experiments, inhibition by PP2 was 28±13% for Pyk2, 80±8% for Src, 71±9%, for Syk and 63±11% for STAT3. The modest inhibition of Pyk2 phosphorylation is consistent with the ability of Src to activate Pyk2 (ref. 40), and suggests feedback amplification of Pyk2 activation by Src. The less than complete inhibition of Syk and STAT3 phosphorylation could be due to the ~20% residual Src activity. Alternatively, a Src-independent link between Pyk2 and Syk–STAT3 might exist. PP2 inhibited CpG-driven IgG

secretion by $70\pm12\%$ ($n = 3$, $P < 0.05$), but had no effect on CD40–IL-21 driven IgG secretion (Fig. 6h). Similar results were obtained with the structurally different Src kinase inhibitor SU6656 (data not shown). Taken together the above results suggest that TLR9 ligation activates a Pyk2-Src-Syk cascade that results in STAT3 phosphorylation.

A DOCK8-MyD88-Pyk2 complex links to Lyn

Our results place DOCK8 and Pyk2 downstream of MyD88. To examine whether DOCK8 associates with MyD88, 293T cells were co-transfected with vectors encoding Myc-tagged DOCK8 and HA-tagged MyD88, or HA-tagged myocardin-related transcription factor-A (MRTF-A) as a control. DOCK8 was found to co-precipitate with MyD88, but not with MRTF-A (Fig. 7a). To examine whether DOCK8 associates with MyD88 in B cells, DOCK8 immunoprecipitates from normal EBV-B cells were probed for MyD88. DOCK8 associated weakly with MyD88 in unstimulated cells, but this association increased following CpG stimulation (Fig. 7b).

Pyk2 was reported to interact with MyD88 in macrophages[41]. This interaction was mapped to the proline-rich C-terminal region of Pyk2 and the death domain of MyD88. Probing of MyD88 immunoprecipitates from normal EBV-B cells with mAb to Pyk2 revealed that Pyk2 associates with MyD88 (Fig. 7c). This association was not altered detectably by CpG stimulation and was independent of DOCK8, as Pyk2 co-precipitated with MyD88 from lysates of EBV-B cells from DOCK8-deficient patients (Fig. 7c). Pyk2 was readily detected in DOCK8 immunoprecipitates from normal EBV-B cells (Fig. 7d). This association increased following CpG stimulation. The constitutive association of DOCK8 and Pyk2 was independent of MyD88 and was observed in EBV-B cells from a MyD88-deficient patient that express no detectable MyD88 protein (Fig. 7d). However, CpG stimulation did not increase the association of DOCK8 and Pyk2 in the absence of MyD88. These results suggest that DOCK8 forms a complex with MyD88 and Pyk2.

The YEEVK motif (amino acids 628–632) in the DHR1 domain of DOCK8 also exists in cofilin-1 where it is a target of Pyk2 phosphorylation[42]. This motif is located within a sequence in DOCK8 (HNKSPDFYEEVKIKL, amino acids 621–635), which is a potential binding site for the SH2 domain of Src. Probing DOCK8 immunoprecipitates from EBV-B cells with mAbs to phosphotyrosine and Src revealed that CpG stimulation caused tyrosine phosphorylation of DOCK8 and its association with Src (Fig. 7e). Both events were abrogated by the Pyk2 inhibitor Tyrphostin A9. The Src family member Lyn is expressed preferentially in B cells[43]. Probing Lyn immunoprecipitates with a pY416Src mAb demonstrated that CpG stimulation causes tyrosine phosphorylation of Lyn in normal B cells (Fig. 7f). Furthermore, CpG stimulation caused robust association of Lyn with DOCK8, which was abrogated by addition of the Pyk2 inhibitor Tyrphostin A9 (Fig. 7g). These results indicate that TLR9 ligation in B cells causes Pyk2-dependent DOCK8 phosphorylation and recruitment of Src and/or Lyn.

DISCUSSION

We present evidence that DOCK8 functions as an adaptor that links TLR9 via MyD88 to a Pyk2-Src-Syk-STAT3 signaling cascade, and we demonstrate that this pathway is essential for TLR9-driven B cell proliferation and immunoglobulin production.

DOCK8-deficient patients had impaired ability to sustain a protective antibody response, similar to DOCK8 mutant mice, and lacked circulating CD27^{+} memory B cells. DOCK8-deficient B cells failed to proliferate and secrete IgM and IgG in response to CpG. This defect is cell-autonomous, specific to CpG and not accounted for by the lack of memory B cells. Because of constraints in obtaining sufficient amounts of blood from children for B

cell purification, our experiments used PBMCs, which were stimulated with the B cell selective TLR9 ligand CpG ODN2006, and/or EBV-B cells. Whenever possible, purified B cells from at least two patients were also used.

CpG stimulation normally upregulated the expression of *AICDA*, CD23 and CD86 in DOCK8-deficient B cells and resulted in normal activation of NF-κB and p38, and normal IRF7-dependent secretion of IFN-α in DOCK8-deficient PBMCs, indicating that these events occur independently of DOCK8. Unexpectedly, given the reported GEF activity of DOCK proteins for small GTPases[21], CpG activated Rac1 independently of DOCK8. CpG activation of Rac1 in pDCs uses a non-TLR9 sensor and DOCK2 (ref. 34). A similar pathway could be operative in B cells.

A central finding in this study is that CpG causes STAT3 phosphorylation in B cells in a DOCK8-dependent manner. Impaired STAT3 phosphorylation in DOCK8-deficient B cells was specific for CpG stimulation, and was not secondary to the lack of memory B cells. The critical role of STAT3 in CpG-driven B cell proliferation and differentiation was demonstrated by the observation that these responses were impaired in patients with dominant-negative mutations in *STAT3*. The failure of IL-6, which caused STAT3 phosphorylation in DOCK8-deficient B cells, to correct their defective response to CpG indicates that other DOCK8-dependent signals are also required for CpG-driven B cell proliferation and IgG secretion. These may include signals delivered by Pyk2, Src and Syk which trigger the activation of phospholipase C-γ, phosphatidylinositol-3-OH kinase and B cell linker protein (BLNK)[44–46].

Syk was shown to play a critical role in CpG-driven STAT3-dependent B cell proliferation and differentiation. CpG stimulation of B cells caused Syk phosphorylation, which was severely impaired in DOCK8-deficient B cells, placing Syk downstream of DOCK8. The Syk selective inhibitor SYKINH-61 blocked CpG-driven STAT3 phosphorylation, placing Syk upstream of STAT3, and inhibited CpG-driven B cell proliferation and IgG secretion. CpG stimulation of B cells caused DOCK8-dependent phosphorylation of Pyk2 and Src. DOCK8 was demonstrated to link TLR9-MyD88 to a Pyk2-Src-Syk-STAT3 cascade in B cells, which was shown to be essential for TLR9-driven B cell activation. The observation that CpG-driven phosphorylation of Pyk2, Src, Syk and STAT3, and B cell proliferation and differentiation were dependent on TLR9 and MyD88, indicate that CpG engagement of TLR9-MyD88 results in DOCK8-dependent B cell activation. CpG-A DNA has been reported to induce tyrosine phosphorylation of proteins, including Syk, in monocytes and macrophages independently of TLR9 and MyD88 (ref. 47). Differences in the ODNs and target cells used may account for the difference in the requirement for TLR9 and MyD88.

DOCK8 was found to exist in a complex with MyD88 and Pyk2. MyD88 was not essential for DOCK8-Pyk2 association, and DOCK8 was not essential for MyD88-Pyk2 association, although it was essential for Pyk2 phosphorylation following TLR9 ligation. Following CpG stimulation, DOCK8 became more strongly associated with MyD88 and Pyk2, underwent tyrosine phosphorylation and associated with Src and/or Lyn. We propose the following model of DOCK8 dependent TLR9 signaling. Ligation of TLR9 by CpG causes recruitment and stabilization of a preexisting MyD88-Pyk2-DOCK8 complex, which results in autophosphorylation and activation of Pyk2. Pyk2 then phosphorylates DOCK8 causing it to recruit Src kinases, including Lyn, via their SH2 domain, releasing them from auto-inhibition. Src then activates Syk, which drives STAT3 activation. The proposed pathway is likely a simplification. Src and Syk can phosphorylate Pyk2 (ref. 40), and Src and Pyk2 can synergize to cause STAT3 phosphorylation[48, 49]. Future experiments will determine whether the DOCK8-dependent TLR9-MyD88 signaling pathway we have identified is used by other

receptors that signal via MyD88 in B cells and other cells. Preliminary data indicates that this pathway is activated by TLR4 ligation in PBMCs (data not shown).

DOCK8 deficiency results in impaired immunological synapse in B cells[22] and may impair the ability of T cells and DCs to drive antibody production by B cells. Mice with selective DOCK8 deficiency in B cells, and mice in which the interaction between MyD88 and DOCK8 is disrupted will help define the contribution of DOCK8-dependent MyD88 signaling in B cells to the impaired serologic memory in DOCK8 deficiency. Given that TLR9 ligands are vaccine adjuvants and the role of TLR9 in autoantibody responses to self DNA[50], the TLR9 signaling pathway we have described may be important for developing better vaccines and understanding and treating autoantibody-mediated diseases.

Methods

Patients

Ten patients with established *DOCK8* mutations and six with *STAT3* mutations were studied. Informed consent was provided by adult donors or by the children's parents or guardian. Protocols used in the human studies have been approved by the Committee on Clinical Investigations at Children's Hospital, Boston, MA, USA.

Cell preparation

Human PBMCs were isolated from heparinized blood obtained from patients and normal donors using Ficoll-Hypaque (GE Healthcare). Naïve and total B cells were purified from PBMCs by negative selection using the B cell isolation Kits II (Miltenyi Biotec) according to the manufacturer's recommendation and contained >96% CD19$^+$ cells. Cells were suspended in RPMI-1640 containing 10% heat-inactivated FCS (Hyclone), 2 mM L-glutamine, 50 µg/ml streptomycin and 100 U/ml penicillin (medium). Epstein-Barr virus (EBV) transformed cell lines on patients and controls were established as described[51].

Cell cultures

PBMCs (1×10^6 and 1.5×10^6 cells/ml for proliferation and immunoglobulin production respectively) or B cells (1.5×10^6 cells/ml) were cultured with medium, CpG ODN 2006 or 2216 (0.1 µM, Invivogen), or anti-CD40 (5 µg/ml, clone 626.1) in the presence of either recombinant (r) human interleukin 21 (IL-21, (50 ng/ml, Miltenyi Biotech), or rIL-4 (5 ng/ml, R&D Systems). The following kinase inhibitors were used: Syk inhibitor (SYKINH-61, a kind gift of F. Uckun, University of Southern California, Los Angeles); Pyk2 inhibitor (Tyrphostin A9, AG 17), and Src inhibitor (PP2) from EMD biosciences. Proliferation was assayed 4 days later by assaying for ^{3}H-thymidine incorporation. IgM, IgG and IgE production was measured in 14-day culture supernatants by ELISA as previously described[52]. CpG-mediated upregulation of CD23 and CD86 expression was analyzed by flow cytometry after 48 h. IL-6 and IFN-α in culture supernatants were measured after 24 h using ELISA kits from Invitrogen. Apoptosis was evaluated on day 3 after stimulation. IgM specific tetanus toxoid (TT) antibody in sera was assayed using ELISA kit from IBL International.

Flow cytometry

Anti-human monoclonal antibodies to the following were used for staining: CD3 (HIT3a), CD19 (HIB19), CD27 (M-T271), CD23 (M-L233), CD86 (2331(FUN-1)) and IgD (IA6-2) (BD Biosciences); CD123 (AC145) and BDCA-4 (AD5-17F6) (Miltenyi) with the appropriate isotype controls. Annexin V–FITC was purchased from Biovision Inc. Data collected with a FACSCalibur cytometer (BD Biosciences) were analyzed with CellQuest software (BD Biosciences) or FlowJo software (TreeStar).

Quantitative-PCR (Q-PCR)

RNA was extracted from cultured B cells on day 5 using TRIzol (Invitrogen) and was reverse transcribed by Supercript II RT (Invitrogen) according to manufacturer's instructions. Q-PCR for *AICDA* was performed using primers and an ABI Prism 7300 sequence detector from Applied Biosystems. Relative RNA expression normalized to GAPDH RNA abundance was calculated by the relative standard curve method as outlined in the manufacturer's technical bulletin (Applied Biosystems).

Immunoblot analysis

PBMCs, B cells or EBV-transformed B cell lines (1×10^6 cells/condition) were unstimulated or stimulated with either CpG (2.5 μM), IL-21 (10 ng/ml), IFN-α (1000 U/ml), Biosource), rIL-6 (2 ng/ml, R&D systems) or anti-human IgM (10 μg/ml, Jackson Immuno Research Labs). Total cell lysates were then separated by SDS-PAGE gel electrophoresis and transferred to nitrocellulose membranes. The following antibodies were used for immunoblot analysis: anti-DOCK8 (#HPA003218, Sigma-Aldrich); anti-STAT3 (79D7), anti-BLNK (#3587), anti-Pyk2 (5E2), anti-Lyn (C13F9) and antibodies to phosphorylated p38 (D3F9), IκBα (ser32/36, 5A5), STAT3 (Tyr705, D3A7), Syk (Tyr352, #2701), Pyk2 (Tyr402, #3291), and Src family (Tyr416, #2101) (Cell Signaling); anti-IκBα (sc-847), anti-IKKγ (Fl-419), and anti-HA (Santa Cruz Biotechnology); anti-Syk (4D10.1), anti-Src (CT, NL19), anti-Myc (9E10), and anti-phosphotyrosine (4G10) (Millipore). The densitometric analysis of the scanned bands was evaluated using the NIH Image program J 1.440 software.

Transient Transfections and Co-Immunoprecipitation

A wild-type human DOCK8 construct was generated with a Myc tag by PCR amplification of pCR4-TOPO human DOCK8 cDNA (Open Biosystems) using standard cloning techniques. 293T cells were transfected with plasmids encoding Myc-tagged DOCK8, HA-tagged MyD88, and HA-tagged MRTF-A (R. Treisman, Cancer Research, UK), using Lipofectamine LTX (Invitrogen). After 16 h, cells were lysed with buffer containing 0.75% NP-40. Immunoprecipitation was performed using a monoclonal anti-HA (HA-7) agarose conjugate (Sigma-Aldrich), were separated by SDS-PAGE, transferred to nitrocellulose membranes, and immunoblotted with antibodies against Myc, MyD88 and HA. For immunoprecipitation (IP) experiments in EBVs, IP and MyD88 blotting was done with anti-MyD88 (H00004615-PW2 pair, Novus).

Rac1 precipitation assay

RAC1 activation was assessed by pull-down from lysates with a fusion protein of gluthatione-S-transferase and the PBD domain of PAK1 (Pierce Laboratories) as previously described[53]. Immunoblot of precipitated samples and aliquots of the cell extracts for loading controls was then performed with RAC1 antibody (Pierce Laboratories).

Subcellular localization of TLR9 in CpG stimulated B cells

EBV transformed B cells stimulated with CpG for 90 min, were spun onto poly-D-lysine-coated coverslips (50 μg/ml, Sigma). Localization of TLR9 to endoplasmic reticulum was confirmed using ER Tracker® Red marker and Alexa 488-conjugated (green) anti-TLR9 (26C593.2, Imgenex Corp). Cells were loaded with ER Tracker® Red (Invitrogen) per vendor's protocol, fixed in 4% paraformaldehyde, permeabilized with 0.04% saponin in 1% BSA[54] and incubated with anti-TLR9. Coverslips were mounted on slides using Prolong Gold with DAPI antifade mounting medium (Invitrogen). Cells on coverslips were fixed in 4% paraformaldehyde, permeabilized with 0.25% Triton X-100, blocked with 10% FCS in PBS, incubated with Early endosome (EEA1, 1G11) and late endosomes/lysosomes (LAMP1, H4A3) monoclonal antibodies (Abcam) for 1 h at 25°C, washed and stained with

Alexa 555-conjugated (red) anti-mouse IgG (Invitrogen). Counterstaining with TLR9 antibody and slide mounting was performed as described above. All images were acquired using a Nikon Eclipse Ti inverted microscope, and were processed using NIS elements AR3.0 software and/or Adobe Photoshop.

Short hairpin RNA (shRNA)- mediated Knockdown (KD) of Pyk2 and Syk expression in CH12 cells

pGIPZ lentiviral vectors encoding green fluorescent protein (GFP) as well as shRNAs specific for murine Pyk2, Syk and a non-silencing (NS, scrambled) plasmid were purchased from Open Biosystems. CH12 cells were transfected by electroporation with 0.5 µg/ml of each plasmid and transduced cells were selected using puromycin. GFP-positive cells were subcloned and tested for Pyk2 and Syk protein expression by immunoblotting.

Mice

TLR9- and Myd88-deficient and the corresponding C57BL/6 and BALB/c wild-type control mice were used at 8–12 weeks of age according to the guidelines of the Animal Care Committee of Children's Hospital, Harvard Medical School, Boston, MA, USA.

Mouse Cell cultures

B cells were purified from splenic cell suspensions by negative selection using CD43-conjugated magnetic beads from Miltenyi. Purified B cells (>95% B220$^+$) were suspended in complete medium containing 50 µM β-mercaptoethanol and were cultured (10^6 cells/ml) with medium or CpG ODN 1826 (3 µg/ml, Invivogen). Proliferation was assayed day 4 by measuring ^{3}H-thymidine incorporation. Day 6 IgG was measured in culture supernatants by ELISA. For immunoblot studies CpG ODN 1826 (2.5 µM) and mouse rIL-21 (10 ng/ml, R&D Systems) were used.

Statistical analysis

Student t-test was used for statistical analysis.

Supplementary Material

Refer to Web version on PubMed Central for supplementary material.

Acknowledgments

References

1. Yoshida T, et al. Memory B and memory plasma cells. Immunol Rev. 2010; 237:117–139. [PubMed: 20727033]

2. Huggins J, et al. CpG DNA activation and plasma-cell differentiation of CD27- naive human B cells. Blood. 2007; 109:1611–1619. [PubMed: 17032927]

3. Jiang W, et al. TLR9 stimulation drives naive B cells to proliferate and to attain enhanced antigen presenting function. Eur J Immunol. 2007; 37:2205–2213. [PubMed: 17621369]

4. Giordani L, et al. IFN-alpha amplifies human naive B cell TLR-9-mediated activation and Ig production. J Leukoc Biol. 2009; 86:261–271. [PubMed: 19401392]

5. Carpenter EL, Mick R, Ruter J, Vonderheide RH. Activation of human B cells by the agonist CD40 antibody CP-870,893 and augmentation with simultaneous toll-like receptor 9 stimulation. J Transl Med. 2009; 7:93. [PubMed: 19906293]

6. Katsenelson N, et al. Synthetic CpG oligodeoxynucleotides augment BAFF- and APRIL-mediated immunoglobulin secretion. Eur J Immunol. 2007; 37:1785–1795. [PubMed: 17557373]

7. Weeratna RD, Makinen SR, McCluskie MJ, Davis HL. TLR agonists as vaccine adjuvants: comparison of CpG ODN and Resiquimod (R-848). Vaccine. 2005; 23:5263–5270. [PubMed: 16081189]

8. Zhang XQ, et al. Potent antigen-specific immune responses stimulated by codelivery of CpG ODN and antigens in degradable microparticles. J Immunother. 2007; 30:469–478. [PubMed: 17589287]

9. Cunningham-Rundles C, Bodian C. Common variable immunodeficiency: clinical and immunological features of 248 patients. Clin Immunol. 1999; 92:34–48. [PubMed: 10413651]

10. Latz E, et al. Ligand-induced conformational changes allosterically activate Toll-like receptor 9. Nat Immunol. 2007; 8:772–779. [PubMed: 17572678]

11. Pasare C, Medzhitov R. Control of B-cell responses by Toll-like receptors. Nature. 2005; 438:364–368. [PubMed: 16292312]

12. Guay HM, Andreyeva TA, Garcea RL, Welsh RM, Szomolanyi-Tsuda E. MyD88 is required for the formation of long-term humoral immunity to virus infection. J Immunol. 2007; 178:5124–5131. [PubMed: 17404295]

13. Hou B, et al. Selective Utilization of Toll-like Receptor and MyD88 Signaling in B Cells for Enhancement of the Antiviral Germinal Center Response. Immunity. 2011; 34:375–384. [PubMed: 21353603]

14. Meyer-Bahlburg A, Khim S, Rawlings DJ. B cell intrinsic TLR signals amplify but are not required for humoral immunity. J Exp Med. 2007; 204:3095–3101. [PubMed: 18039950]

15. Gavin AL, et al. Adjuvant-enhanced antibody responses in the absence of toll-like receptor signaling. Science. 2006; 314:1936–1938. [PubMed: 17185603]

16. Park SM, et al. MyD88 signaling is not essential for induction of antigen-specific B cell responses but is indispensable for protection against Streptococcus pneumoniae infection following oral vaccination with attenuated Salmonella expressing PspA antigen. J Immunol. 2008; 181:6447–6455. [PubMed: 18941235]

17. Seibert SA, Mex P, Kohler A, Kaufmann SH, Mittrucker HW. TLR2-, TLR4-and Myd88-independent acquired humoral and cellular immunity against Salmonella enterica serovar Typhimurium. Immunol Lett. 2010; 127:126–134. [PubMed: 19895846]

18. Sin JI. MyD88 signal is required for more efficient induction of Ag-specific adaptive immune responses and antitumor resistance in a human papillomavirus E7 DNA vaccine model. Vaccine. 2011; 29:4125–4131. [PubMed: 21496466]

19. Browne EP, Littman DR. Myd88 is required for an antibody response to retroviral infection. PLoS Pathog. 2009; 5:e1000298. [PubMed: 19214214]

20. Meller N, Merlot S, Guda C. CZH proteins: a new family of Rho-GEFs. J Cell Sci. 2005; 118:4937–4946. [PubMed: 16254241]

21. Cote JF, Vuori K. GEF what? Dock180 and related proteins help Rac to polarize cells in new ways. Trends Cell Biol. 2007; 17:383–393. [PubMed: 17765544]

22. Randall KL, et al. Dock8 mutations cripple B cell immunological synapses, germinal centers and long-lived antibody production. Nat Immunol. 2009; 10:1283–1291. [PubMed: 19898472]

23. Zhang Q, et al. Combined immunodeficiency associated with DOCK8 mutations. N Engl J Med. 2009; 361:2046–2055. [PubMed: 19776401]

24. Engelhardt KR, et al. Large deletions and point mutations involving the dedicator of cytokinesis 8 (DOCK8) in the autosomal-recessive form of hyper-IgE syndrome. J Allergy Clin Immunol. 2009; 124:1289–1302. e1284. [PubMed: 20004785]

25. Bonilla FA, et al. Practice parameter for the diagnosis and management of primary immunodeficiency. Ann Allergy Asthma Immunol. 2005; 94:S1–63. [PubMed: 15945566]

26. Broder K, et al. Preventing tetanus, diphtheria, and pertussis among adolescents: use of tetanus toxoid, reduced diphtheria toxoid and acellular pertussis vaccines recommendations of the Advisory Committee on Immunization Practices (ACIP). MMWR Recomm Rep. 2006; 55:1–34.

27. Hartmann G, et al. Delineation of a CpG phosphorothioate oligodeoxynucleotide for activating primate immune responses in vitro and in vivo. J Immunol. 2000; 164:1617–1624. [PubMed: 10640783]

28. Cunningham-Rundles C, et al. TLR9 activation is defective in common variable immune deficiency. J Immunol. 2006; 176:1978–1987. [PubMed: 16424230]

29. Hartmann G, Krieg AM. Mechanism and function of a newly identified CpG DNA motif in human primary B cells. J Immunol. 2000; 164:944–953. [PubMed: 10623843]

30. Dedeoglu F, Horwitz B, Chaudhuri J, Alt FW, Geha RS. Induction of activation-induced cytidine deaminase gene expression by IL-4 and CD40 ligation is dependent on STAT6 and NFkappaB. Int Immunol. 2004; 16:395–404. [PubMed: 14978013]

31. Arrighi JF, Rebsamen M, Rousset F, Kindler V, Hauser C. A critical role for p38 mitogen-activated protein kinase in the maturation of human blood-derived dendritic cells induced by lipopolysaccharide, TNF-alpha, and contact sensitizers. J Immunol. 2001; 166:3837–3845. [PubMed: 11238627]

32. Lim W, et al. Distinct role of p38 and c-Jun N-terminal kinases in IL-10-dependent and IL-10-independent regulation of the costimulatory molecule B7.2 in lipopolysaccharide-stimulated human monocytic cells. J Immunol. 2002; 168:1759–1769. [PubMed: 11823508]

33. Kawai T, et al. Interferon-alpha induction through Toll-like receptors involves a direct interaction of IRF7 with MyD88 and TRAF6. Nat Immunol. 2004; 5:1061–1068. [PubMed: 15361868]

34. Gotoh K, et al. Selective control of type I IFN induction by the Rac activator DOCK2 during TLR-mediated plasmacytoid dendritic cell activation. J Exp Med. 2010; 207:721–730. [PubMed: 20231379]

35. Avery DT, et al. B cell-intrinsic signaling through IL-21 receptor and STAT3 is required for establishing long-lived antibody responses in humans. J Exp Med. 2010; 207:155–171. [PubMed: 20048285]

36. Diehl SA, et al. STAT3-mediated up-regulation of BLIMP1 Is coordinated with BCL6 down-regulation to control human plasma cell differentiation. J Immunol. 2008; 180:4805–4815. [PubMed: 18354204]

37. Barton GM, Kagan JC. A cell biological view of Toll-like receptor function: regulation through compartmentalization. Nat Rev Immunol. 2009; 9:535–542. [PubMed: 19556980]

38. Matsuda T, Hirano T. Association of p72 tyrosine kinase with Stat factors and its activation by interleukin-3, interleukin-6, and granulocyte colony-stimulating factor. Blood. 1994; 83:3457–3461. [PubMed: 7515712]

39. Uckun FM, Qazi S, Ma H, Tuel-Ahlgren L, Ozer Z. STAT3 is a substrate of SYK tyrosine kinase in B-lineage leukemia/lymphoma cells exposed to oxidative stress. Proc Natl Acad Sci USA. 2010; 107:2902–2907. [PubMed: 20133729]

40. Avraham H, Park SY, Schinkmann K, Avraham S. RAFTK/Pyk2-mediated cellular signalling. Cell Signal. 2000; 12:123–133. [PubMed: 10704819]

41. Xi CX, Xiong F, Zhou Z, Mei L, Xiong WC. PYK2 interacts with MyD88 and regulates MyD88-mediated NF-kappaB activation in macrophages. J Leukoc Biol. 2010; 87:415–423. [PubMed: 19955209]

42. Bonnette PC, et al. Phosphoproteomic characterization of PYK2 signaling pathways involved in osteogenesis. J Proteomics. 2010; 73:1306–1320. [PubMed: 20116462]

43. Gauld SB, Cambier JC. Src-family kinases in B-cell development and signaling. Oncogene. 2004; 23:8001–8006. [PubMed: 15489917]

44. Haynes MP, et al. Src kinase mediates phosphatidylinositol 3-kinase/Akt-dependent rapid endothelial nitric-oxide synthase activation by estrogen. J Biol Chem. 2003; 278:2118–2123. [PubMed: 12431978]

45. Boudot C, et al. Involvement of the Src kinase Lyn in phospholipase C-gamma 2 phosphorylation and phosphatidylinositol 3-kinase activation in Epo signalling. Biochem Biophys Res Commun. 2003; 300:437–442. [PubMed: 12504103]

46. Mocsai A, Ruland J, Tybulewicz VL. The SYK tyrosine kinase: a crucial player in diverse biological functions. Nat Rev Immunol. 2010; 10:387–402. [PubMed: 20467426]

47. Sanjuan MA, et al. CpG-induced tyrosine phosphorylation occurs via a TLR9-independent mechanism and is required for cytokine secretion. J Cell Biol. 2006; 172:1057–1068. [PubMed: 16567503]

48. Turkson J, et al. Stat3 activation by Src induces specific gene regulation and is required for cell transformation. Mol Cell Biol. 1998; 18:2545–2552. [PubMed: 9566874]

49. Shi CS, Kehrl JH. Pyk2 amplifies epidermal growth factor and c-Src-induced Stat3 activation. J Biol Chem. 2004; 279:17224–17231. [PubMed: 14963038]

50. Green NM, Marshak-Rothstein A. Toll-like receptor driven B cell activation in the induction of systemic autoimmunity. Semin Immunol. 2011; 23:106–112. [PubMed: 21306913]

51. Jabara HH, Fu SM, Geha RS, Vercelli D. CD40 and IgE: Synergism between anti-CD40 mAb and IL-4 in the induction of IgE synthesis by highly purified human B cells. J Exp Med. 1990; 172:1861–1864. [PubMed: 1701824]

52. Jabara HH, Brodeur SR, Geha RS. Glucocorticoids upregulate CD40 ligand expression and induce CD40L-dependent immunoglobulin isotype switching. J Clin Invest. 2001; 107:371–378. [PubMed: 11160161]

53. Gallego MD, et al. WIP and WASP play complementary roles in T cell homing and chemotaxis to SDF-1α. Int Immunol. 2006; 18:221–232. [PubMed: 16141245]

54. Shen XZ, Lukacher AE, Billet S, Williams IR, Bernstein KE. Expression of angiotensin-converting enzyme changes major histocompatibility complex class I peptide presentation by modifying C termini of peptide precursors. J Biol Chem. 2008; 283:9957–9965. [PubMed: 18252713]
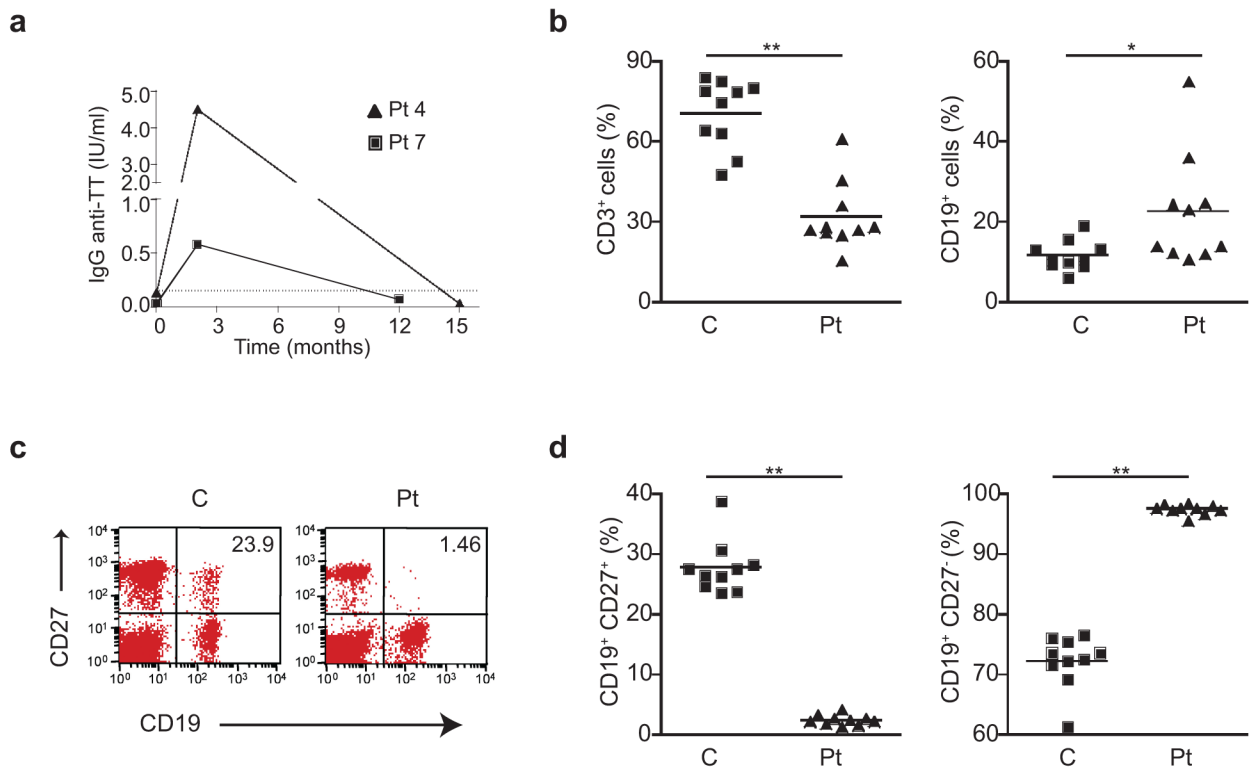
Figure 1. Impaired antibody responses, failure to maintain serologic memory and decreased memory B cells in DOCK8 deficient patients

(a) Serial antibody titers after re-immunization with TT in two DOCK8 deficient patients aged 8 (Pt. 4) and 15 years (Pt. 7). The dotted line represents the lower limit of the protective antibody titer. **(b)** Percentage of $CD3^+$ (T) cells and $CD19^+$ (B) cells in PBMCs from DOCK8 deficient patients (Pt) and controls (C **(c)** Representative flow cytometry analysis of CD19 and CD27 expression by PBMCs from DOCK8 deficient patients and controls. **(d)** Percentage of $CD27^+$ memory B cells and $CD27^-$ naïve B cells in the $CD19^+$ B cell population of DOCK8 deficient patients and controls. Each symbol (**b,d**) represents an individual subject; small horizontal lines indicate the mean. *$P<0.05$ and **$P<0.001$ (Student's t-test).
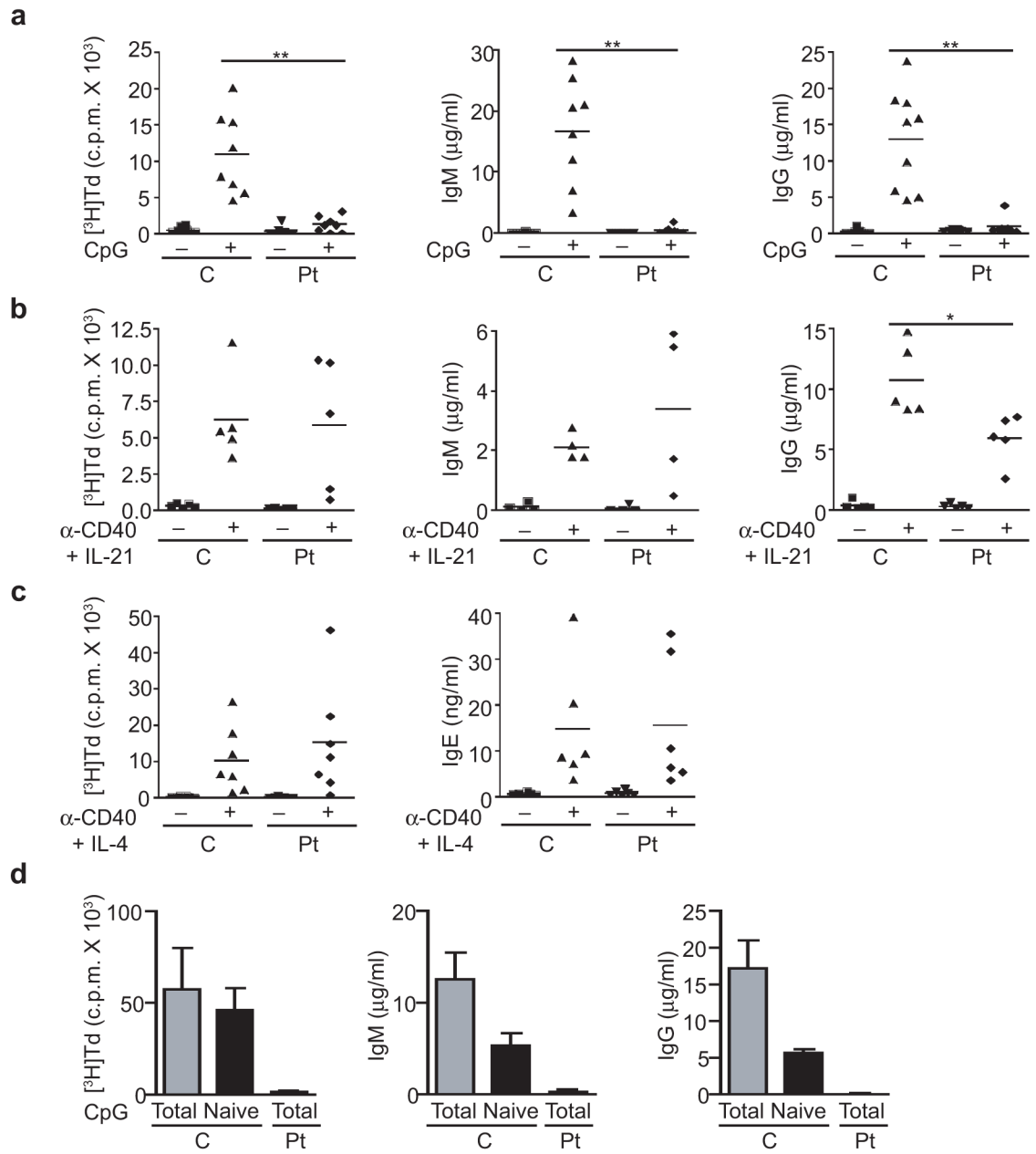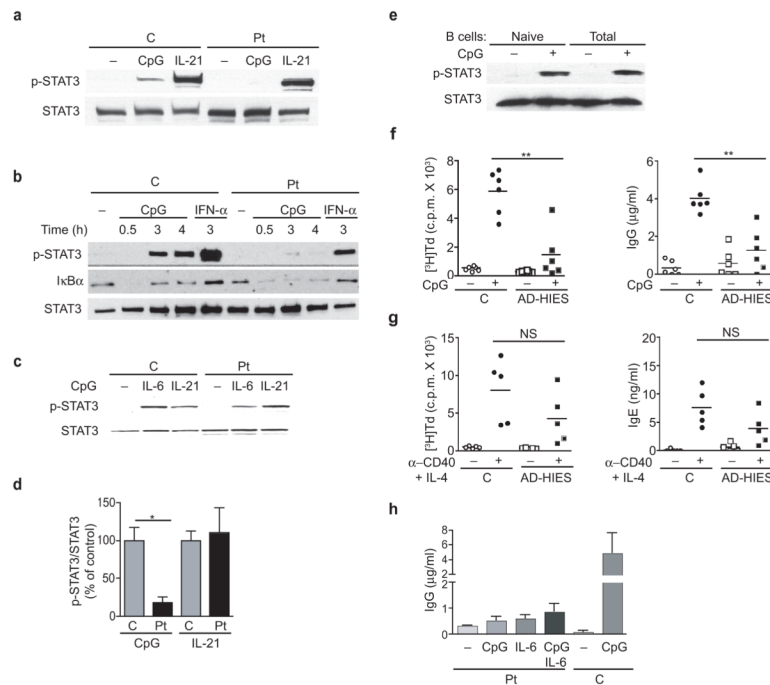
Figure 2. Impaired CpG driven B cell proliferation and immunoglobulin (Ig) production to CpG in DOCK8 deficient patients
(a–c) Proliferation and Ig secretion by PBMCs from DOCK8 deficient patients (Pt) and controls (C) in response to stimulation with CpG **(a)**, anti-CD40 + IL-21 **(b)** and anti-CD40 + IL-4 **(c).** Not all 10 patients could be studied in each assay. **(d)** Proliferation, and secretion of IgM and IgG by highly purified total and naïve B cells from controls (n=3 each) and purified total B cells from DOCK8 deficient patients (n=2 each) in response to stimulation with CpG (mean and s.e.). Each symbol (**a,b,c**) represents an individual subject; small horizontal lines indicate the mean. *P<0.05, and **P<0.001 (Student's t-test).
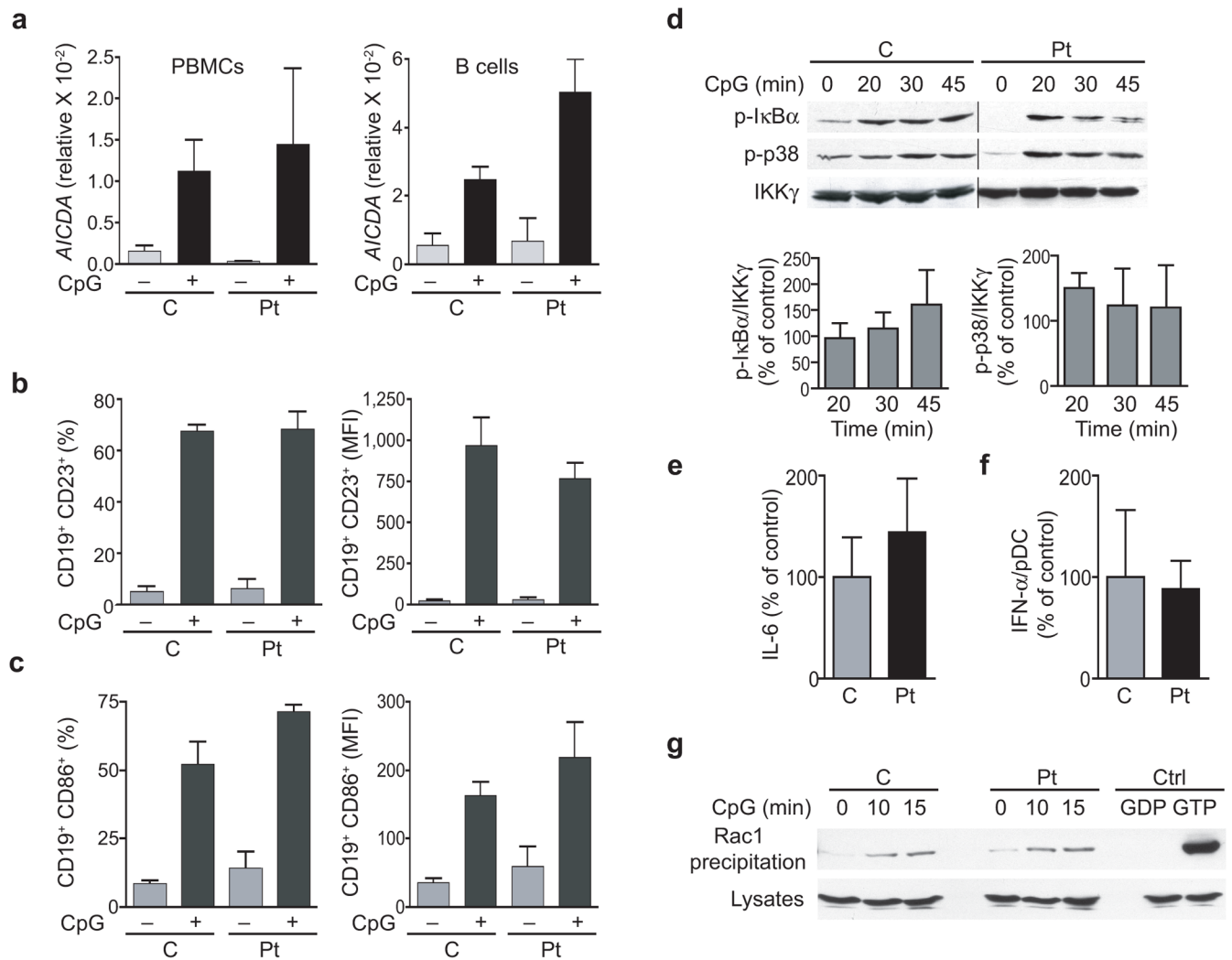
**Figure 3. Normal CpG-driven upregulation of *AICDA,* CD23 and CD86 expression, activation of NFκB, p38 MAP kinase and Rac1, and IL-6 secretion in B cells from DOCK8 deficient patients**
(a) CpG-induced expression of mRNA for *AICDA* in PBMCs (left) and purified B cells (right) from patients and controls (n= 2 each). **(b,c)** Percentage of CD19^{+} B cells expressing surface CD23 and CD86 (left), and their MFI (right) before and after CpG stimulation of PBMCs from patients and controls (n=3 each). **(d)** Representative (top) and quantitation (expressed in lower panels as percent of control, n=3 each) of CpG-driven phosphorylation of IκBα and p38 in PBMCs from patients and controls. IKKγ was used as loading control. **(e)** CpG-driven IL-6 secretion by EBV-B cells from patients relative to controls (n=3 each, mean for controls 55 pg/ml). **(f)** IFN-α secretion by pDCs in PBMCs from patients and controls in response to stimulation with CpG-A ODN 2216 (n=3 each, mean for controls 22.4 pg/100 pDCs). The number of pDCs/culture was calculated from the percentage of CD123^{+}BDCA-4^{+} cells in each sample. **(g)** CpG-driven Rac1 activation in EBV-B cells determined by a GST-PAK precipitation assay followed by immunoblotting for Rac1. Equal volume aliquots of the lysates used in the pull-down assay were immunoblotted for Rac1 as loading controls. Similar data was obtained on three different patients and controls in **g**; (mean and s.e. in **a–f**).

Figure 4. CpG-induced DOCK8 dependent STAT3 phosphorylation in B cells is essential for B cell proliferation and IgG production

(a,b) CpG-driven STAT3 Y705 phosphorylation in PBMCs **(a)** and purified B cells **(b)** from DOCK8 deficient patients and controls. **(c)** IL-6 and IL-21 driven STAT3 Y705 phosphorylation in B cells from DOCK8 deficient patients. **(d)** Quantitation of CpG- and IL-21-driven STAT3 Y705 phosphorylation in B cells from DOCK8 deficient patients and controls (n=3 each). pSTAT3 and STAT3 bands were scanned by densitometry and the pSTAT3/STAT3 ratio was calculated and expressed relative to the mean pSTAT3/STAT3 ratio in controls, which was arbitrarily set at 100% (n=3 per group). **(e)** CpG-driven STAT3 phosphorylation in total B cells and naïve B cells purified from the same donor. **(f,g)** CpG-driven proliferation and Ig secretion (n=6 each) **(f)**, and CD40/IL-4 driven proliferation and IgE secretion (n=5 each) **(g)**, by PBMCs from STAT3 deficient AD-HIES patients and controls. **(h)** Effect of IL-6 (2 ng/ml) on CpG driven IgG secretion by PBMCs from DOCK8 deficient patients (n=3). Results are representative of three patients and three controls in **a** and **b**, and three controls in **e**; mean and s.e. (**d, h**) and small horizontal lines indicate the mean (**f, g**). NS, not significant; *P<0.01 and **P<0.001 (Student's t-test).
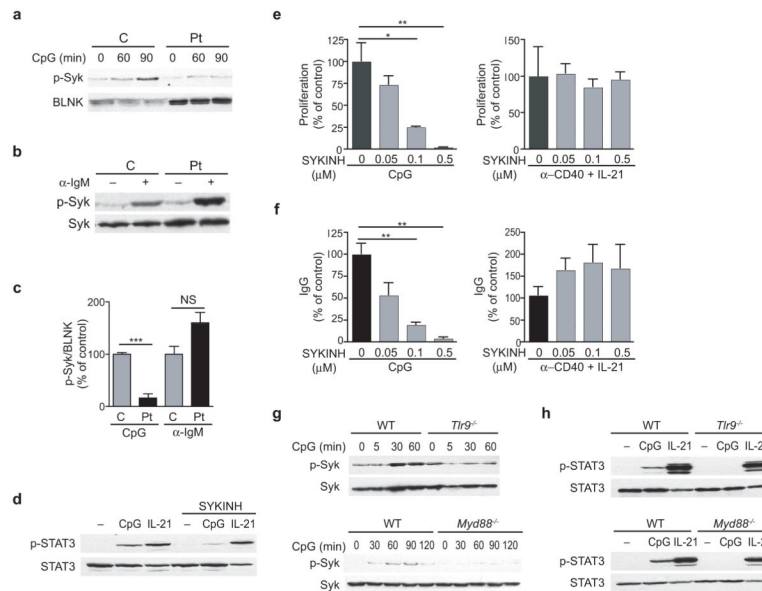
Figure 5. CpG-driven phosphorylation of STAT3 in B cells is dependent on Syk, and requires TLR9 and MyD88

(a,b) Syk phosphorylation following CpG stimulation **(a)** and anti-IgM stimulation **(b)** of normal and DOCK8 deficient PBMCs detected by immunoblotting with anti-pY352Syk. **(c)** Quantitation of CpG-driven and BCR-driven Syk Y352 phosphorylation in PBMCs from DOCK8 deficient patients and controls. pSyk and BLNK bands were scanned by densitometry and the pSyk/BLNK ratio was calculated and expressed relative to the mean pSyk/BLNK ratio in controls, which was arbitrarily set at 100% (n=3 per group). **(d)** Effect of the Syk inhibitor SYKINH-61 on CpG-driven STAT3 Y705 phosphorylation in normal PBMCs. IL-21 driven STAT3 phosphorylation was used as a control. Results are representative of three independent experiments. **(e,f)** Effect of SYKINH-61 on CpG-driven and CD40 + IL21-driven proliferation **(e)**, IgG production **(f)** by normal PBMCs (n=4). **(g,h)** CpG-driven Syk Y352 and STAT3 Y705 phosphorylation in splenic B cells from $Tlr9^{-/-}$ mice and C57BL/6 WT controls **(g)**, and from $Myd88^{-/-}$ mice and BALB/c WT controls **(h)**. Mean and s.e. (**c, e–f**); NS, not significant; *$P<0.05$, **$P<0.01$, and ***$P<0.001$ (Student's t-test).
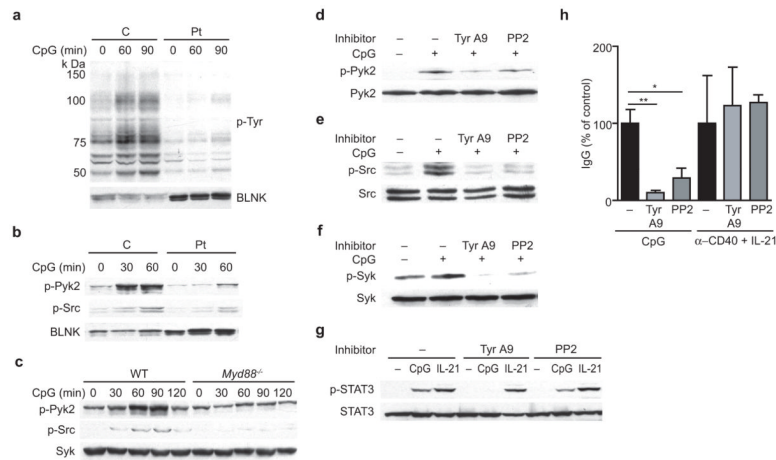
Figure 6. DOCK8 mediates CpG activation of a Pyk2-Src-Syk-STAT3 cascade essential for B cell proliferation and differentiation

(a,b) Representative immunoblot analysis of lysates from CpG-stimulated PBMCs from a DOCK8 deficient patient and a normal control for tyrosine phophorylated proteins **(a)** and for phosphorylation of Pyk2 at Y402 and Src at Y416 **(b)**. BLNK was used as loading control. The higher amounts of BLNK in PBMCs from the patients reflect the higher percentage of CD19^{+} B cells in the patients compared to controls (23% versus 7 % in **a** and 19% versus 8% in **b** respectively). **(c)** Immunoblot analysis of lysates from CpG-stimulated splenic B cells from $Myd88^{-/-}$ mice and BALB/c WT controls for pY402Pyk2 and pY416Src. **(d–g)** Effect of the Pyk2 inhibitor tyrphostin A9 (Tyr A9) and the Src kinase inhibitor PP2 on CpG-driven phosphorylation of Pyk2 at Y402 **(d)**, Src at Y416 **(e)**, Syk Y352 **(f)**, and STAT3 at Y705 **(g)** in normal PBMCs. **(h)** Effect of Tyr A9 and PP2 on CpG-driven IgG secretion by normal PBMCs. Stimulation with anti-CD40+IL-21 was used as control. Results in **(a–g)** are representative of three independent experiments. Data in **(h)** represent mean and s.e. of three experiments. *P<0.05 and **P<0.01 (Student's t-test).
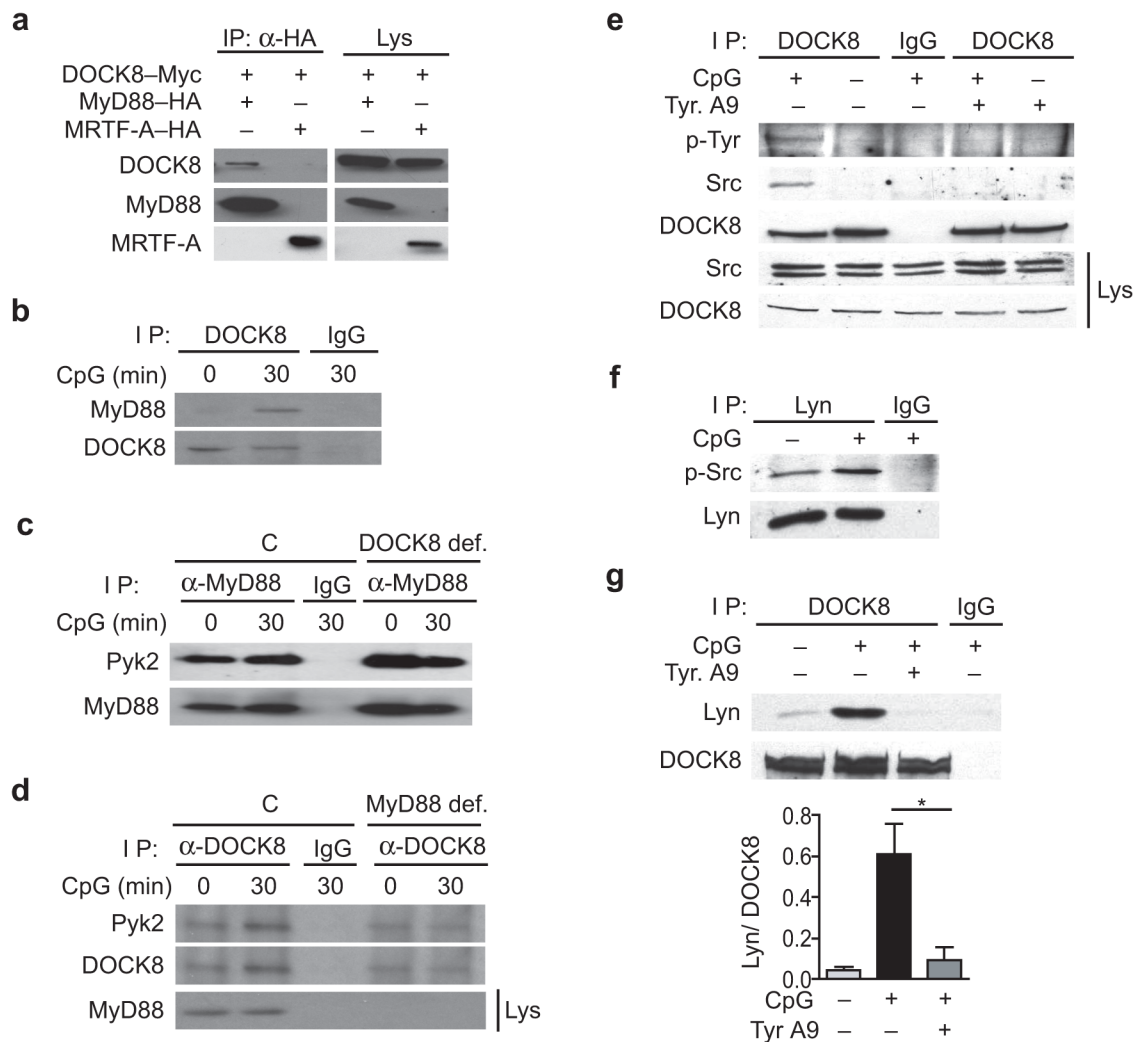
Figure 7. DOCK8 associates with MyD88 and Pyk2 and undergoes Pyk2-mediated tyrosine phosphorylation and association with Src/Lyn following TLR9 ligation
(a,b) Association of DOCK8 with MyD88 in 293T cell transfectants **(a)** and in EBV-B cells **(b). (c,d)** Association of Pyk2 and MyD88 in EBV-B cells from control (C) and DOCK8 deficient (def) patient **(c)** and of Pyk2 and DOCK8 EBV-B cells from control (C) and MyD88 def patient **(d)**. Results in **a–d** are representative of three experiments. **(e)** DOCK8 tyrosine phosphorylation and association with Src following CpG stimulation of normal B cells. DOCK8 immunoprecipates were probed with anti-p-Tyr, anti-Src and anti-DOCK8 as loading control. Equal volumes of lysates were probed for Src and DOCK8. **(f)** CpG- driven Lyn phosphorylation in normal PBMCs. Lyn immunopreciptates were probed with anti-pY416Src and with anti-Lyn as loading control. **(g)** Lyn recruitment to DOCK8 following CpG stimulation of normal PBMCs with CpG. DOCK8 immunoprecipitates were probed with anti-Lyn and anti-DOCK8 as loading control. Upper panel: representative experiment. Lower panel: quantitative analysis of the lyn/DOCK8 band intensity ratio (n=3, mean and s.e.).

Table 1

IgG antibody titers in immunized DOCK8 deficient patients

	% with protective antibody titer			
	TT	HepB	HiB	PV
DOCK8-deficient patients ($n = 5$)	40%	0%	20%	20%
Normal children (n= see legend)	>99%	>99%	83–97%	50–100%

Frequency of protective IgG antibody titers to TT, HepB, HiB, and PV in five immunized DOCK8-deficient patients who received a full course of immunization with the vaccines, compared to published values in normal controls cited in Ref. 25 and the vaccine prescribing information. The numbers of normal children were 3,032 for TT, 147 for HepB, 3,486 for HiB and 18,906 for PV. Antibody titers were obtained prior to replacement with gammaglobulin. Values for protective antibody titers were provided by the clinical laboratory where the test was performed.